Theoretical Study on the Mechanism of Iron Carbonyls Mediated Isomerization of Allylic Alcohols to Saturated Carbonyls

Vicenç Branchadell,*[a] Christophe Crévisy,[b] and René Grée*[b]

Abstract: The conversion of allylic alcohols to enols mediated by $Fe(CO)_3$ has been studied through density functional theoretical calculations. From the results obtained a complete catalytic cycle has been proposed in which the first intermediate is the [(allyl alcohol)$Fe(CO)_3$] complex. This intermediate evolves to the [(enol)$Fe(CO)_3$] complex through two consecutive 1,3-hydrogen shifts involving a π-allyl hydride intermediate. The highest Gibbs energy transition state corresponds to the partial decoordination ot the enol ligand prior to the coordination of a new allyl alcohol molecule that regenerates the first intermediate. Alternative processes for the [(enol)$Fe(CO)_3$] complex such as [$Fe(CO)_3$]-mediated enol–aldehyde transformation and enol isomerization have also been considered. The results obtained show that the former process is unfavourable, whereas the enol isomerization may compete with the enol decoordination step of the catalytic cycle.

Keywords: allylic compounds · density functional calculations · homogeneous catalysis · iron carbonyls · isomerization

Introduction

The conversion of allylic alcohols to saturated carbonyls is a useful synthetic process usually requiring a two-step sequence of oxidation (reduction) followed by reduction (oxidation). A one-pot catalytic transformation by an internal redox type process (Scheme 1) is an attractive alternative strategy: It resembles a complete atom economy process, which also minimizes the number of protection–deprotection steps often required for such transformations.[1, 2]

Around 50 transition-metal catalysts, prepared from ten different metals have been already used in this isomerization. Essentially two different mechanisms have been proposed for this reaction. They strongly depend upon the nature of the catalyst and involve either metal-hydride or π-allyl intermediates.[1b, 1c, 3] Iron carbonyls were among the first catalysts reported for this transformation[4] and later studies have delineated the scope and limitations of their use in organic synthesis, with respect to the allylic alcohol substrate.[5] From a mechanistic point of view, it has been demonstrated that various iron carbonyl derivatives such as [$Fe(CO)_5$], [$Fe_2(CO)_9$], [$Fe_3(CO)_{12}$] as well as [(bda)$Fe(CO)_3$] could be used as catalysts, affording good evidence that [$Fe(CO)_3$] would act as the true catalytic species.[4–6] Elegant labeling studies have also established that the reaction involved a 1,3-shift from the hydrogen on the carbinol center onto the γ carbon and that this transfer was intramolecular.[7] Furthermore, exploiting the known topology of dihydrocyclopentadienes, it was also demonstrated that the migrating H must be close to the reactive iron carbonyl.[8] The latter result gave good indication for a reaction occuring in the coordination sphere of the metal, even if for allylic alcohols the kinetic isotope effect studies afforded values lower than those observed for normal alkenes.[9] All these data appear in good agreement with the generally accepted mechanism (Scheme 2).[1b, c, 3]

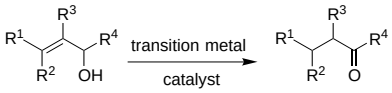

Scheme 1.

[a] Dr. V. Branchadell
Departament de Química
Universitat Autònoma de Barcelona, Edifici Cn
08193 Bellaterra (Spain)
Fax: (+34) 935812920
E-mail: vicenc.branchadell@uab.es

[b] Dr. R. Grée, Dr. C. Crévisy
ENSCR, Laboratoire de Synthèses
et Activations de Biomolécules, CNRS UMR 6052
Avenue du Général Leclerc
35700 Rennes Beaulieu (France)
Fax: (+33) 2-23-23-81-08
E-mail: rene.gree@ensc-rennes.fr

The reaction of allylic alcohols with the iron carbonyl catalyst leads first to a η^2 alkene complex **A**. Then migration of the hydrogen linked to the carbinol center onto the metal affords a π-allyl iron hydride intermediate **B**. Readdition of this hydrogen on the other side of the allylic alcohol affords the η^2 enol **C**. A final decomplexation regenerates the catalyst and gives the enol which tautomerises to the corresponding carbonyl compound. It has to be noted that this is only an

DOI: 10.1002/chem.200204567

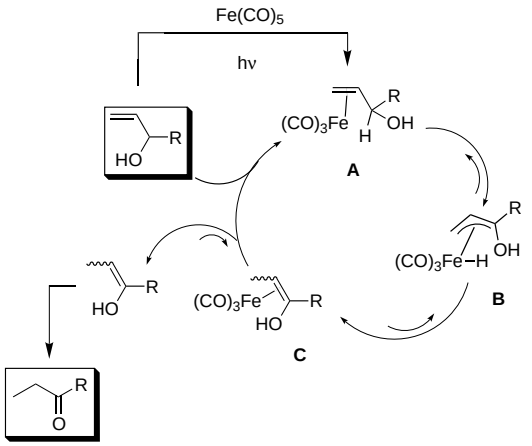

Scheme 2.

extension of the mechanism proposed for the known hydrogen migration in alkenes mediated by iron carbonyls.[10] The main difference, however, is that the product which is obtained (here an enol) tautomerises to the carbonyl, to afford an irreversible step in the reaction pathway.

This mechanism globally accounts for all data but leaves open some important questions such as the position of the highest energy transition state on the reaction pathway and its exact structure. Furthermore, the detailed mechanism of the last step (**C**–**A**) is a key issue for the knowledge of the catalytic cycle; at this stage, dissociative as well as associative mechanisms could be envisaged.

The purpose of this paper is to report, for the first time, an extensive theoretical study of this isomerization reaction. Using allyl alcohol as a simple model, high level computational studies have provided structural information on all intermediates involved in this process, as well as on the transition states. From the results obtained a complete catalytic cycle has been proposed.

Computational Methods

All geometries have been fully optimized using the B3LYP[11] density functional method implemented in the Gaussian 98 program.[12] Energy minima and transition states have been optimized by means of the standard Schlegel algorithm using redundant internal coordinates.[13] Harmonic vibrational frequencies have been computed for all structures to characterize them as energy minima (all frequencies are real) or transition states (one and only one imaginary frequency). In the geometry optimizations we have used the LANL2DZ basis set.[14] This is a double-ζ basis set for C, O and H and for the valence space of Fe whereas the inner shells of Fe (up to 2p) are represented by an effective core potential. This basis set has been supplemented with a set of d polarization functions for C and O with exponents 0.75 and 0.85, respectively.

Energies of all stationary points have been recalculated through single point calculations using the 6-311+G(d,p)[15] basis set. For Fe it involves a triple-ζ basis set with a set of f polarization functions. The reported energies have been calculated with the larger basis set whereas zero-point and thermal corrections to the energy and entropies at 1atm and 298.15 K have been obtained from vibrational frequencies computed with the LANL2DZ basis set.

Results and Discussion

The photodissociation of $[Fe(CO)_5]$ can lead to the formation of $[Fe(CO)_4]$ and $[Fe(CO)_3]$.[16] The π complexation of olefins by these iron carbonyls is a well established process, affording η^4 and/or η^2 complexes.[17] As we have mentioned in the introduction, $[Fe(CO)_3]$ is very likely the species involved in the catalytic process. The structures of the complexes corresponding to the coordination of allyl alcohol to the iron carbonyls are shown in Figure 1. The iron tetracarbonyl

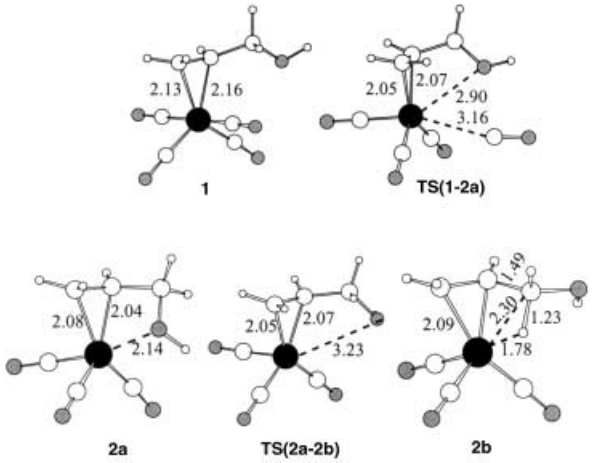

Figure 1. Structures of the [(allyl alcohol)$Fe(CO)_4$] (**1**) and [(allyl alcohol)$Fe(CO)_3$] (**2a** and **2b**) complexes and of transition states corresponding to Fe–CO bond dissociation and conformational changes. Selected interatomic distances in Å.

complex **1** presents a trigonal-bipyramid structure with the olefin in one of the equatorial positions, in excellent agreement with the experimental gas phase structure of the [(ethylene)$Fe(CO)_4$] complex.[18] The computed Fe–olefin bond dissociation energies are 24.4 kcal mol^{-1} for **1** and 26.2 kcal mol^{-1} for [(ethylene)$Fe(CO)_4$]. The latter value is smaller than the experimental estimate of 36 ± 4 kcal mol^{-1}.[19] The computed values correspond to the spin-allowed processes which lead to the formation of singlet $Fe(CO)_4$, which is 8.9 kcal mol^{-1} higher in energy than the triplet ground state at the same level of calculation.

Two different conformers, **2a** and **2b** for the iron-tricarbonyl complexes are shown in Figure 1. These are 16e species that are stabilized by interactions involving the alcohol oxygen atom (**2a**) or one of the C–H bonds (**2b**). We have also located the transition state corresponding to the **2a**,**b** conformational change. Table 1 presents the relative energies and Gibbs energies of all these structures. As we can observe, the most stable conformer of the iron tricarbonyl complex is **2a**. The computed Fe–olefin bond dissociation energy for this complex is 43.5 kcal mol^{-1}, so that the Fe–olefin bond in **2a** is notably stronger than in the iron tetracarbonyl complex. This value is notably larger than the experimental estimate of 20–25 kcal mol^{-1} for the [(1-pentene)$Fe(CO)_3$] complex.[20] For this system we have computed Fe–olefin bond dissociation energy and the obtained value is 34.7 kcal mol^{-1}.

Table 1. Relative energies and Gibbs energies for the stationary points corresponding to the formation and conformational changes of the [(allyl alcohol)$Fe(CO)_3$] complex.[a]

	ΔE [kcal mol^{-1}]	ΔG^0_{298} [kcal mol^{-1}]
	1 → **2a**+CO	
TS(1-2a)	28.9	24.5
2a+CO	24.4	9.2
	2a → **2b**	
TS(2a-2b)	12.6	11.1
2b	7.8	6.4

[a] See Figure 1.

The formation of **2a** from **1** by Fe–CO bond dissociation is endothermic with a reaction energy of 24.4 kcal mol^{-1}. This value is notably lower than the experimental first bond dissociation energy of $[Fe(CO)_5]$, 42 ± 2 kcal mol^{-1}.[21] The computed value for this process is 38.0 kcal mol^{-1}.

Compound **2a** is the most stable structure of the [(allyl alcohol)$Fe(CO)_3$] complex. However, **2b** has a more appropriate geometry to allow hydrogen migration onto the metal. The **2a**, **b** rearrangement involves a rotation around a C–C bond and the computed Gibbs activation energy is 11.1 kcal mol^{-1}. Compound **2b** presents a β-agostic interaction involving one of the C–H bonds. The values of Fe–C, Fe–H, and C–H distances are in the range of values observed for this kind of interaction.[22]

At this stage, migration of the hydrogen onto the metal leading to the formation of the π-allyl hydride intermediate becomes possible. The structures of the stationary points involved in this process are shown in Figure 2 and the corresponding relative energies and Gibbs energies are presented in Table 2.

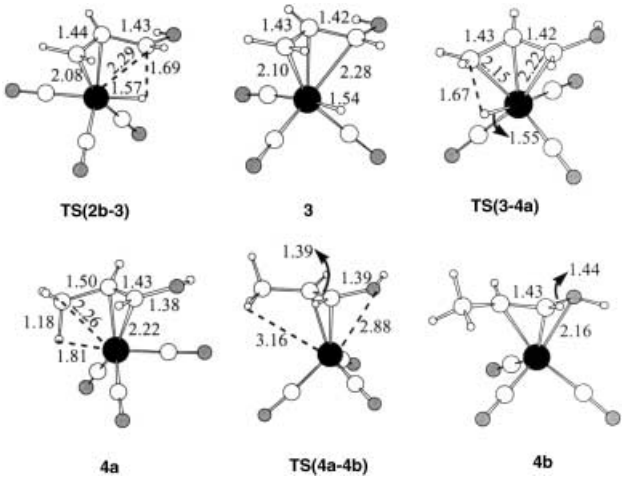

Figure 2. Structures of the stationary points corresponding to the isomerization of allyl alcohol to enol mediated by $[Fe(CO)_3]$. Selected interatomic distances in Å.

The computed Gibbs activation energy for the formation of the π-allyl hydride intermediate **3** is 3.8 kcal mol^{-1}, so that this process is expected to be very fast.[20] At the transition state between **2b** and **3** the Fe–H distance is very close to the value corresponding to **3**, but the C–H bond has not been completely broken yet. The value of the Fe–H bond length

Table 2. Relative energies and Gibbs energies for the stationary points corresponding to the isomerization of the allyl alcohol in the presence of $[Fe(CO)_3]$.[a]

	ΔE [kcal mol^{-1}]	ΔG^0_{298} [kcal mol^{-1}]
2b	0.0	0.0
TS(2b-3)	5.1	3.8
3	−3.0	−3.7
TS(3-4a)	8.0	6.5
4a	−1.6	−2.1
TS(4a-4b)	5.9	4.1
4b	−4.3	−4.1

[a] See Figure 2.

of **3** is slightly smaller than the experimental value corresponding to $H_2Fe(CO)_4$.[23]

The next step in the isomerization mechanism is a hydrogen shift onto the terminal carbon with a concomitant reorganisation at the metal centre to give **4a** (see Figure 2 and Table 2). This process is slower than the first hydrogen shift, in such a way that the transition state between **3** and **4a** becomes the highest energy transition state along the isomerization reaction path. Compound **4a** presents a C–H agostic interaction. The values of the geometry parameters associated to this interaction show that it is weaker than for **2b**. The value of the Fe–H distance at the transition state **TS(3-4a)** is very similar to the value corresponding to **3**.

From the η^2 complex **4a** a final reorganisation around the metal centre occurs to give the η^3 complex **4b** which is slightly more stable. Therefore, **4b** may be considered as a key intermediate in the isomerization process. Starting from **2a** the activation Gibbs energy for the complete process towards **4b** is 12.9 kcal mol^{-1} with the highest point being between **3** and **4a**. Such a relatively low Gibbs activation energy strongly suggests that all the processes between **2a** and **4b** should be reversible.

In order to complete the catalytic cycle for the isomerization, a decoordination process has to be found for the enol. The Fe-enol bond dissociation energy for **4b** is 34.9 kcal mol^{-1}. This bond is weaker than the Fe-allyl alcohol bond in **2a** (43.5 kcal mol^{-1}). The ΔG corresponding to the dissociation of **4b** into $Fe(CO)_3$ and free enol is 18.6 kcal mol^{-1}. This value provides an upper limit for the activation Gibbs energy for a decoordination step.

Starting from the key intermediate **4b** two different decoordination paths, either associative or dissociative, have been considered. The transition states and intermediates corresponding to these two reaction paths are represented in Figure 3 and the corresponding relative energies and Gibbs energies are shown in Table 3.

The direct addition of allyl alcohol on **4b** (path I) induces a decoordination of the oxygen atom of the enol ligand to give intermediate **5a** where both the enol and the allyl alcohol are bonded in a η^2 mode. The activation Gibbs energy for this process is 12.2 kcal mol^{-1}.

The values of the Fe–C distances show that **5a** presents a very weak enol–Fe interaction. When the enol ligand is moved away, the energy monotonously increases to yield the [(allyl alcohol)$Fe(CO)_3$] complex **2c**. So, there is not a transition state on the potential energy surface for this

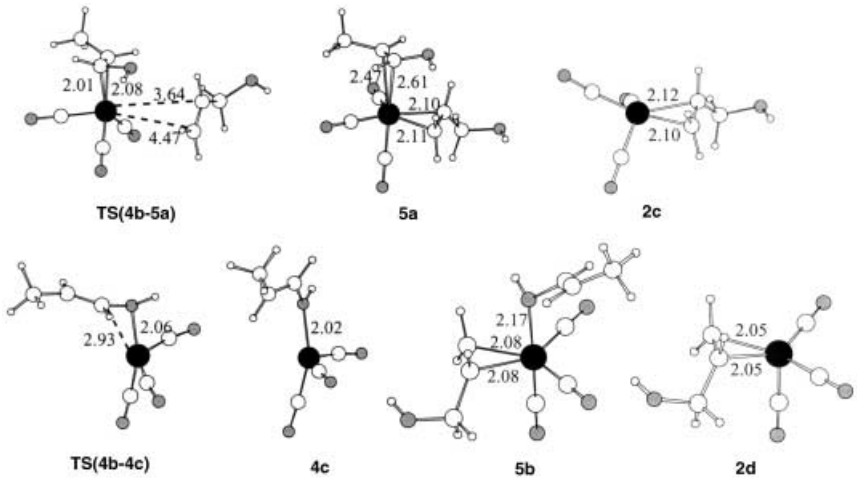

Figure 3. Structures of the stationary points corresponding to the enol decoordination from $[Fe(CO)_3]$ in the mechanism of allyl alcohol isomerization. Selected interatomic distances in Å.

Table 3. Energies and Gibbs energies relative to **4b** and allyl alcohol for the enol decoordination step.[a]

	ΔE [kcal mol^{-1}]	ΔG^0_{298} [kcal mol^{-1}]
	path I	
TS(4b-5a)	2.0	12.2
5a	−6.2	8.4
2c+enol	2.6	1.5
TS(2c-2a)	2.9	1.8
2a	−9.5	−8.7
	path II	
TS(4b-4c)	12.8	11.3
4c	10.7	8.2
5b	−10.7	1.6
2d+enol	1.5	0.1
TS(2d-2b)	3.6	2.8
2b	0.3	−2.3
TS(2b-2a)	3.6	5.0
2a	−7.5	−8.7

[a] See Figure 3.

process. The inclusion of entropy makes the process thermodynamically favourable, with a ΔG of −6.9 kcal mol^{-1}. Compound **2c** can easily rearrange through a rotation around the C–C bond to the most stable conformer **2a** with a Gibbs activation energy of only 0.3 kcal mol^{-1}. It has to be noticed that the activation Gibbs energy for the whole associative process (**4b**–**2a**) is 12.2 kcal mol^{-1} and that ΔG is −8.7 kcal mol^{-1}. On the other hand, the enol would tautomerize to the corresponding carbonyl. The computed ΔG for the enol–propanal transformation is −10.5 kcal mol^{-1}.

The first step of path II involves a decoordination of the C=C double bond of the enol ligand affording the intermediate **4c** where the enol is σ-bonded to the iron tricarbonyl unit. For this dissociative process the transition state is very close to **4c** and the corresponding Gibbs activation energy is 11.3 kcal mol^{-1}.

Allyl alcohol coordinates to **4c** without any potential energy barrier yielding the intermediate **5b**, where the allyl alcohol is η^2 bonded to iron while the enol is σ bonded through the oxygen lone pair. The Gibbs reaction energy corresponding to this process is −6.6 kcal mol^{-1}. The decoordination of the enol from **5b** takes place without a transition state leading to the formation of **2d**. This process is endothermic by 12.2 kcal mol^{-1}, but the inclusion of entropy leads to a ΔG of −1.5 kcal mol^{-1}. Compound **2d** is a minimum on the potential energy surface of the [(allyl alcohol)$Fe(CO)_3$] complex that can easily rearrange to **2b** and finally to the most stable conformer **2a**.

The comparison of the results obtained for the two decoordination pathways shows that, at least on this simple model, path II ($\Delta G^{\neq} = 11.3$ kcal mol^{-1}) is slightly more favourable than path I ($\Delta G^{\neq} = 12.2$ kcal mol^{-1}). However, the difference is too small to completely discard path I.

The decoordination of the enol ligand is not the only possible reaction which has to be considered for **4b**. By analogy with the isomerization process described previously, it was proposed earlier that the hydroxyl hydrogen could migrate onto the metal to give a hetero π-allyl transition metal hydride. Then a second migration onto the carbon atom would give the corresponding carbonyl coordinated to the catalyst (Scheme 3).[24]

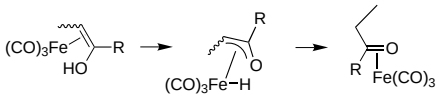

Scheme 3.

Such a mechanism was proposed for the Rh^I-catalyzed isomerization of allylic alcohols and it could explain why some asymmetric induction was observed when optically active ligands were introduced on these catalysts.[24]

We have studied this kind of process for the iron carbonyl mediated isomerization of allyl alcohol. The structures of the transition states and intermediates involved in this process are shown in Figure 4 and the corresponding relative energies and Gibbs energies are presented in Table 4.

The transfer of hydrogen from **4b** leads to the formation of the oxoallyl iron hydride complex **6**. The activation Gibbs energy of this process, 20.0 kcal mol^{-1}, is much higher than the values computed for the alternative processes. At the transition state **TS(4b-6)** the Fe–H distance is larger than for other transition states involved in hydrogen transfers from C–H bonds such as **TS(2b-3)** and **TS(3-4a)** (Figure 2).

From **6** a second hydrogen transfer leads to the formation of the [(aldehyde)$Fe(CO)_3$] complex **7** with a $\Delta G^{\neq}$ of 8.5 kcal mol^{-1}. Although the process from **4b** to **7** is thermodynamically favourable ($\Delta G = -11.0$ kcal mol^{-1}) it appears very unlikely for iron carbonyls since it is kinetically much less

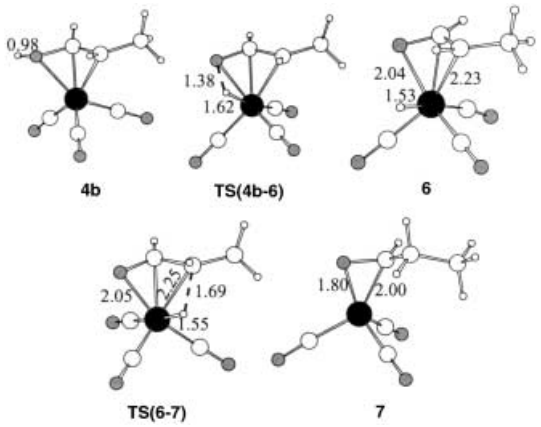

Figure 4. Structures of the stationary points corresponding to enol – aldehyde isomerization mediated by $[Fe(CO)_3]$. Selected interatomic distances in Å.

Table 4. Relative energies and Gibbs energies for stationary points corresponding to the enol – aldehyde isomerization mediated by $[Fe(CO)_3]$.[a]

	ΔE [kcal mol^{-1}]	ΔG^0_{298} [kcal mol^{-1}]
4b	0.0	0.0
TS(4b-6)	23.1	20.0
6	− 2.1	− 4.0
TS(6-7)	7.0	4.5
7	− 10.3	− 11.0

[a] See Figure 4.

favourable than the previously considered decoordination pathways.

For the isomerization of normal alkenes mediated by iron carbonyls it is known that the reaction continues along the chain leading to a mixture of regio- and stereoisomers.[10] This led us to consider also the possibility of 1,3-shifts for the enols complexed to $[Fe(CO)_3]$ (Scheme 4). For that purpose we

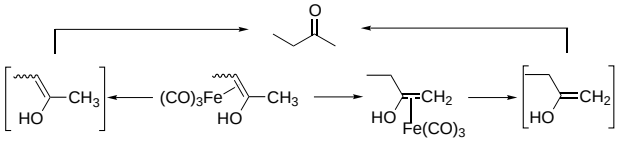

Scheme 4.

have selected the simple model **8a**, similar to **4a** but with an extra methyl vicinal to the OH, and studied its isomerization to complex **10** containing an ethyl chain (Figure 5). The relative energies and Gibbs energies computed for the stationary points corresponding to this process are shown in Table 5.

Compound **8a** is stabilized through a β-agostic interaction involving one of the methyl groups. This complex can easily rearrange to the slightly less stable conformer **8b**, where the agostic interaction involves the methyl group vicinal to OH. From **8b**, the hydrogen transfer onto the metal leads to the π-allyl iron hydride intermediate **9** with an activation Gibbs energy of 8.7 kcal mol^{-1}. From the latter intermediate a second hydrogen transfer occurs leading to **10**, which is the

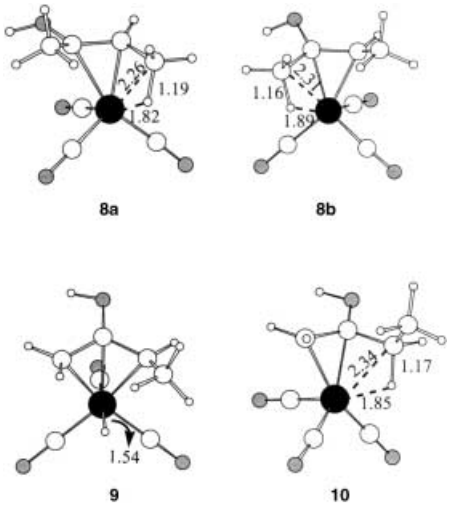

Figure 5. Structures of the stationary points corresponding to enol isomerization mediated by $[Fe(CO)_3]$. Selected interatomic distances in Å.

Table 5. Relative energies and Gibbs energies for stationary points corresponding to enol isomerization mediated by $[Fe(CO)_3]$.[a]

	ΔE [kcal mol^{-1}]	ΔG^0_{298} [kcal mol^{-1}]
8a	0.0	0.0
TS(8a-8b)	5.0	4.3
8b	1.8	1.9
TS(8b-9)	11.9	10.6
9	− 2.4	− 2.6
TS(9-10)	11.4	10.0
10	0.8	0.6

[a] See Figure 5.

transposed enol, complexed to $[Fe(CO)_3]$. The activation Gibbs energy of this type of enol isomerization is of the same order of magnitude (around 10 kcal mol^{-1}) than the values calculated for the allyl alcohol to enol isomerization (**2a** – **4b**). Therefore it appears very likely that all these processes will be in competition. This result would be in agreement with recent experimental data in a novel tandem isomerization – aldolisation reaction mediated by iron carbonyls, since during this reaction not only the expected aldols were obtained but also a small amount of their regioisomers. This was explained by the isomerization of complexed enol intermediates, via such a 1,3-hydrogen shift.[25]

The results obtained for the allyl alcohol to enol isomerization mediated by iron tricarbonyl are summarized in the catalytic cycle shown in Figure 6.

The π complexation of the alcohol with $[Fe(CO)_3]$ leads to the formation of **2a**, which is the first intermediate in the catalytic cycle. After a C–C bond rotation from **2a** to **2b**, hydrogen migration leads to a π-allyl iron hydride **3** intermediate from which a second hydrogen migration affords the η^3 complexed enol **4b**. The attack of a new allyl alcohol molecule to **4b** may lead to the formation of **5b**, where both the enol and the allyl alcohol are coordinated to $[Fe(CO)_3]$. This intermediate is unstable with respect to enol decoordination leading to **2d** which is a conformer of the [(allyl alcohol)$Fe(CO)_3$] complex that easily evolves to the most stable conformer **2a** in two steps. The activation Gibbs

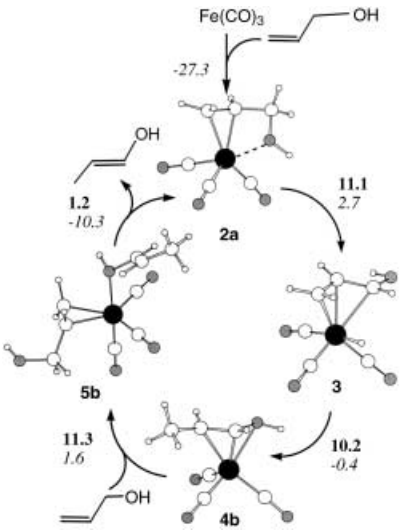

Figure 6. Catalytic cycle corresponding to the isomerization of allyl alcohol to enol mediated by $Fe(CO)_3$. Gibbs activation energies (bold) and Gibbs reaction energies (italics) in kcal mol^{-1}.

energies involved in all steps are low and the highest value, 11.3 kcal mol^{-1}, corresponds to the partial decoordination of the enol ligand from **4b**. Moreover the reaction Gibbs energy of the whole cycle is -6.4 kcal mol^{-1}, corresponding to a slightly exergonic process.

Acknowledgement

This work has been financially supported by DGESIC (Spain) through grant PB98-0912, DGR (Catalonia) through grant 2001SGR-00182 and CNRS (France). Access to the facilities of the Centre de Supercomputació de Catalunya (CESCA) is gratefully acknowledged.

[1] For reviews on the isomerization of allylic alcohols see: a) L. A. Yanovskaya, Kh. Shakhidayatov, *Russ. Chem. Rev.* **1970**, *39*, 859; b) R. C. Van der Drift, E. Bowman, E. Drent, *J. Organomet. Chem.* **2002**, *650*, 1; c) R. Uma, C. Crévisy, R. Grée, *Chem. Rev.* **2003**, *103*, 27.

[2] For a discussion on the atom economy concept see: a) B. M. Trost, *Science* **1991**, *254*, 1471; b B. M. Trost, *Angew. Chem.* **1995**, *107*, 285; *Angew. Chem. Int. Ed. Engl.* **1995**, *34*, 259; c) B. M. Trost, *Acc. Chem. Res.* **2002**, *35*, 695.

[3] a) W. A. Herrmann, in *Applied Homogeneous Catalysis with Organometallic Compounds*, *Vol. 2* (Eds.: B. Cornils, W. A. Herrmann), VCH, Weinheim, **1996**, p. 980; b) S. G. Davies, *Organotransition Metal Chemistry. Applications to Organic Synthesis*, Pergamon (UK), **1982**, p. 266.

[4] G. F. Emerson, R. Pettit, *J. Am. Chem. Soc.* **1962**, *84*, 4591.

[5] a) R. Damico, T. J. Logan, *J. Org. Chem.* **1967**, *32*, 2356; b) H. Cherkaoui, M. Soufiaoui, R. Grée, *Tetrahedron* **2001**, *57*, 2379.

[6] a) N. Iranpoor, H. Imanieh, E. J. Forbes, *Synth. Commun.* **1989**, *19*, 2955; b) N. Iranpoor, E. Mottaghinejad, *J. Organomet. Chem.* **1992**, *423*, 399.

[7] W. T. Hendrix, F. G. Cowherd, J. L. von Rosenberg, *Chem. Commun.* **1968**, 97.

[8] F. G. Cowherd, J. L. von Rosenberg, *J. Am. Chem. Soc.* **1969**, *91*, 2157.

[9] J. U. Strauss, P. W. Ford, *Tetrahedron Lett.* **1975**, *33*, 2917.

[10] T. A. J. Manuel, *J. Org. Chem.* **1962**, *27*, 3941.

[11] a) A. D. Becke, *J. Chem. Phys.* **1993**, *98*, 5648; b) C. Lee, W. Yang, R. G. Parr, *Phys. Rev. B* **1988**, *37*, 785.

[12] *Gaussian 98*, Revision A.5, M. J. Frisch, G. W. Trucks, H. B. Schlegel, G. E. Scuseria, M. A. Robb, J. R. Cheeseman, V. G. Zakrzewski, J. A. Montgomery, Jr., R. E. Stratmann, J. C. Burant, S. Dapprich, J. M. Millam, A. D. Daniels, K. N. Kudin, M. C. Strain, O. Farkas, J. Tomasi, V. Barone, M. Cossi, R. Cammi, B. Mennucci, C. Pomelli, C. Adamo, S. Clifford, J. Ochterski, G. A. Petersson, P. Y. Ayala, Q. Cui, K. Morokuma, D. K. Malick, A. D. Rabuck, K. Raghavachari, J. B. Foresman, J. Cioslowski, J. V. Ortiz, B. B. Stefanov, G. Liu, A. Liashenko, P. Piskorz, I. Komaromi, R. Gomperts, R. L. Martin, D. J. Fox, T. Keith, M. A. Al-Laham, C. Y. Peng, A. Nanayakkara, C. Gonzalez, M. Challacombe, P. M. W. Gill, B. Johnson, W. Chen, M. W. Wong, J. L. Andres, C. Gonzalez, M. Head-Gordon, E. S. Replogle, J. A. Pople, Gaussian, Inc., Pittsburgh PA, **1998**.

[13] C. Peng, P. Y. Ayala, H. B. Schlegel, M. J. Frisch, *J. Comput. Chem.* **1996**, *17*, 49.

[14] a) T. H. Dunning Jr., P. J. Hay, In *Modern Theoretical Chemistry*, *Vol. 3* (Ed.: H. F. Schaeffer III), Plenum, New York, **1976**, p. 1; b) P. J. Hay, W. R. Wadt, *J. Chem. Phys.* **1985**, *82*, 299.

[15] a) R. Krishnan, J. S. Binkley, R. Seeger, J. A. Pople, *J. Chem. Phys.* **1980**, *72*, 650; b) A. J. H. Wachters, *J. Chem. Phys.* **1970**, *52*, 1033; c) P. J. Hay, *J. Chem. Phys.* **1977**, *66*, 4377.

[16] a) L. Bañares, T. Baumert, M. Bergt, B. Kiefer, G. Gerber, *J. Chem. Phys.* **1998**, *108*, 5799; b) O. Rubner, V. Engel, *Chem. Phys. Lett.* **1998**, *293*, 485.

[17] E. A. Koerner von Gustorf, F. W. Grevels, I. Fischler, *The Organic Chemistry of Iron*, *Vol. 1*, Acad. Press, New York, **1978**.

[18] B. J. Drouin, S. G. Kukolich, *J. Am. Chem. Soc.* **1999**, *121*, 4023.

[19] a) D. S. L. Brown, J. A. Connor, M. L. Leung, M. I. Paz Andrade, H. A. Skinner, *J. Organomet. Chem.* **1976**, *110*, 79; b) J. A. Martinho - Simões, J. L. Beauchamp, *Chem. Rev.* **1990**, *90*, 629.

[20] G. T. Long, E. Weitz, *J. Am. Chem. Soc.* **2000**, *122*, 1431.

[21] K. E. Lewis, D. M. Golden, G. P. Smith, *J. Am. Chem. Soc.* **1984**, *106*, 3905.

[22] G. J. Kubas, *Metal Dihydrogen and σ-Bond Complexes. Structure, Theory, and Reactivity*, Kluwer, New York, **2001**.

[23] B. J. Drouin, S. G. Kukolich, *J. Am. Chem. Soc.* **1998**, *120*, 6774.

[24] S. Bergens, B. Bosnich, *J. Am. Chem. Soc.* **1991**, *113*, 958.

[25] C. Crévisy, M. Wietrich, V. Le Boulaire, R. Uma, R. Grée, *Tetrahedron Lett.* **2001**, *42*, 395.

Received: November 8, 2002 [F4567]

